De Novo Ceramide Synthesis Is Required for *N*-Linked Glycosylation in Plasma Cells[1]

Meidan Goldfinger,* Elad L. Laviad,† Rivka Hadar,* Miri Shmuel,* Arie Dagan,‡ Hyejung Park,§ Alfred H. Merrill, Jr.,§ Israel Ringel,* Anthony H. Futerman,† and Boaz Tirosh[2]*

Plasma cells (PCs) are terminally differentiated B lymphocytes responsible for the synthesis and secretion of Igs. The differentiation of B cells into PCs involves a remarkable expansion of both lipid and protein components of the endoplasmic reticulum. Despite their importance in many signal transduction pathways, the role of ceramides, and of complex sphingolipids that are derived from ceramide, in PC differentiation has never been directly studied. To assess their putative role in PC differentiation, we blocked ceramide synthesis with fumonisin B1, a specific inhibitor of ceramide synthase. Under fumonisin B1 treatment, *N*-linked glycosylation was severely impaired in LPS-activated, but not in naive, B cells. We also show that ceramide synthesis is strongly induced by XBP-1 (X box-binding protein-1). In the absence of ceramide synthesis, ER expansion was dramatically diminished. Our results underscore ceramide biosynthesis as a key metabolic pathway in the process of PC differentiation and reveal a previously unknown functional link between sphingolipids and *N*-linked glycosylation in PCs. *The Journal of Immunology,* **2009, 182: 7038–7047.**

Plasma cells (PCs)[3] are terminally differentiated B lymphocytes responsible for the synthesis and secretion of Igs. The differentiation of B cells into PCs involves a series of remarkable phenotypic changes, most prominent of which are a cessation of cell division and remodeling of the secretory pathway (1). IRF4 (IFN regulatory factor 4), Blimp-1, and XBP-1 (X box-binding protein-1) are transcription factors essential for this transition (2–4). While IRF4 and Blimp-1 are required to extinguish the mature B cell program and terminate the germinal center reaction, XBP-1 is required to initiate the PC program, which involves a steep up-regulation of the synthesis of Ig molecules in their secreted form and the expansion of the endoplasmic reticulum (ER) (4–6).

The mechanism behind the expansion of the ER entails a marked increase of both its lipid and protein components (7, 8). These changes are largely regulated by XBP-1 in a process that is sensitive to conditions of ER stress, which ensue when the amount of client proteins that emerge into the ER exceeds its overall folding capacity. XBP-1 is a key element of an intricate cytoprotective ER-to-nucleus signaling pathway, which responds to conditions of ER stress. This pathway is collectively referred to as the unfolded protein response (UPR). The mammalian UPR is composed of at least three transducers: PERK (PKR-like ER kinase), ATF6 (activating transcription factor 6), and IRE1. While PERK reduces protein translation by phosphorylation of eIF2α (eukaryotic initiation factor-2α) on serine 51, ATF6 and IRE1 largely control the transcription of UPR targets. When activated, IRE1 oligomerizes and undergoes autophosphorylation. Phosphorylated IRE1 activates a nuclease activity in its cytosolic tail, which then removes a small intron in the mRNA of XBP-1. The conversion of unspliced XBP-1 (XBP-1u) into the spliced form (XBP-1s) in the course of the UPR yields a potent transcription factor that promotes the transcription of a large number of target genes, whose products participate in almost every aspect of the secretory pathway (9). It is assumed that the steep up-regulation of Ig synthesis to a level that exceeds the folding capacity of the ER in the developing plasma cells induces the UPR, as demonstrated by an increase in ER chaperone synthesis and induction of XBP-1 mRNA splicing (5, 6).

Accordingly, the ectopic expression of XBP-1s in mature B cells, but not the unspliced form of XBP-1, promotes an expansion of the ER (7, 10). As such, overexpression of XBP-1s in fibroblasts is sufficient to increase the ER content (7). These results implicate XBP-1 in its spliced form as a central regulator of ER biogenesis. Biochemical analysis of phospholipid synthesis in fibroblasts revealed that XBP-1 promotes the transcription of cytidine 5′-triphosphate:phosphocholine cytidylyltransferase α (CCTα), the enzyme that catalyzes the rate-limiting step in phosphatidylcholine (PtdCho) synthesis (11). The level of CCTα was also increased in the course of PC differentiation, albeit posttranscriptionally (12).

*Department of Pharmacology and Experimental Therapeutics, School of Pharmacy, The Hebrew University, Jerusalem, Israel; †Department of Biological Chemistry, The Weizmann Institute of Science, Rehovot, Israel; ‡Department of Experimental Medicine and Cancer Research, Hebrew University Medical School, Jerusalem, Israel; and §School of Biology and Petit Institute for Bioengineering and Bioscience, Georgia Institute of Technology, Atlanta, GA 30332

Received for publication September 9, 2008. Accepted for publication April 1, 2009.

The costs of publication of this article were defrayed in part by the payment of page charges. This article must therefore be hereby marked *advertisement* in accordance with 18 U.S.C. Section 1734 solely to indicate this fact.

[1] The study was supported by research grants from the David R. Bloom Center for Pharmacy and Marie-Curie Reintegration Grant 046446 (to B.T.), and from the National Institutes of Health Grant GM076217 (to A.H.M. and A.H.F.). B.T. is affiliated with the David R. Bloom Center for Pharmacy at the Hebrew University (Jerusalem, Israel). A.H.F. is a Joseph Meyerhoff Professor of Biochemistry at the Weizmann Institute of Science.

[2] Address correspondence and reprint requests to Dr. Boaz Tirosh, Department of Pharmacology, School of Pharmacy, Faculty of Medicine, The Hebrew University, Jerusalem 91120, Israel. E-mail address: boazt@ekmd.huji.ac.il

[3] Abbreviations used in this paper: PC, plasma cell; ATF6, activating transcription factor 6; CCTα, cytidine 5′-triphosphate:phosphocholine cytidylyltransferase α; CerS, ceramide synthases; CHX, cycloheximide; ER, endoplasmic reticulum; FB1, fumonisin B1; FSC, forward scatter; KO, knockout; LLO, lipid-linked oligosaccharides; NMR, nuclear magnetic resonance; PERK, PKR-like ER kinase; PtdCho, phosphatidylcholine; SM, sphingomyelin; Tm, tunicamycin; UPR, unfolded protein response; XBP-1, X box-binding protein-1; wt, wild type.

www.jimmunol.org/cgi/doi/10.4049/jimmunol.0802990

These biochemical changes elevate the levels of PtdCho by ~2-fold and thus promote the expansion of the ER. In the liver, XBP-1 is a major lipogenic factor, which positively regulates VLDL secretion. Interestingly, XBP-1 fulfill these tasks without affecting protein secretion, suggesting that in the liver XBP-1 controls a program distinct from that in B cells (13).

Sphingolipids are a highly diverse family of molecules that share a sphingoid long chain base backbone. Central to the sphingolipid metabolic pathway are the ceramides, which serve as precursors to a large number of downstream metabolites. Ceramides are synthesized de novo in the ER by a family of ceramide synthases (CerS) and are further modified in the Golgi apparatus to sphingomyelin (SM) and glycosphingolipids (14). Various stimuli increase ceramide levels, either by promoting their de novo synthesis or by accelerating the hydrolysis of SM to ceramide (reviewed in Ref. 15). The biological function of ceramides has been described mostly in the context of cell survival, as strong promoters of apoptosis and differentiation (16). The mechanism that underlies their proapoptotic function involves activities at both the plasma membrane and mitochondria. Ceramides can exert a direct allosteric effect on enzymes, such as JNK and a kinase suppressor of Ras. When generated at the cell surface, ceramides promote signaling via death receptors (17).

Fumonisins are a group of mycotoxins that are structurally similar to the sphingoid base. Fumonisin B1 (FB1) is a competitive, specific inhibitor of all ceramide synthase isoforms. Incubation with FB1 depletes both ceramides and their downstream metabolites, and therefore is a convenient pharmacological tool to assess the role of sphingolipids in a particular biological process (18, 19).

As part of their maturation, proteins that are targeted to the ER undergo cotranslational *N*-linked glycosylation on asparagine side chains. This modification is recognized by an elaborate quality control system, which assists in glycoprotein folding and has been claimed to serve as a key determinant for sorting of misfolded proteins for degradation (20). More than 20 distinct enzymatic activities cooperate to bring about *N*-linked glycosylation, which includes biosynthesis of dolichol, its substitution with oligosaccharides to yield the lipid-linked oligosaccharides (LLO), transfer of the oligosaccharide to asparagine side chains, and recycling of the dolichol. It has been known for more than 20 years that in the course of PC differentiation, *N*-linked glycosylation is increased by ~25-fold. However, little is known about how *N*-linked glycosylation is regulated in this context (21).

Because of the importance of sphingolipids in many of the signal transduction pathways relevant to PC differentiation, we hypothesized that sphingolipids may modulate the process of PC differentiation. Here, we show that ceramide biosynthesis is up-regulated in the course of PC differentiation in an XBP-1-dependent manner and results in a significant increase in the steady-state levels of sphingolipids. SM levels were elevated relative to other phospholipids, including PtdCho. Moreover, inhibition of de novo ceramide biosynthesis with FB1 abolished the typical ER expansion in the course of PC differentiation. Surprisingly, *N*-linked glycosylation was severely impaired in a dose-dependent manner to a level that resembled a tunicamycin (Tm)-imposed block. This effect was partially rescued by addition of exogenous short acyl-chain ceramide. In contrast to Tm, FB1 affected *N*-linked glycosylation in LPS-activated B cells, but not in freshly harvested splenic B cells. Our results underscore the importance of ceramide biosynthesis as a key metabolic pathway in the process of PC differentiation and reveal a previously unknown link between sphingolipids and *N*-linked glycosylation in PCs.

Materials and Methods

Materials and Abs

FB1 and Tm were purchased from Fermentek. Both compounds were dissolved in DMSO and added at the indicated concentrations. The final DMSO concentration did not exceed 0.5% (v/v). LPS was purchased from Sigma-Aldrich. Endoglycosidase H (EH) was from NEB and used according to the manufacturer's instructions. All solvents were of analytical grade. Goat anti-mouse μ- and κ-chains were from SouthernBiotech. Rabbit polyclonal Ab against H-2K and p97 were provided by Dr. H. Ploegh (Whitehead Institute, Cambridge, MA). C6-ceramide and C8-ceramide were provided by Dr. Y. Barenholz (The Hebrew University of Jerusalem, Jerusalem, Israel).

Mice

Mice on a mixed 129/C57BL background containing a conditional floxed allele to XBP-1 (XBP-$1^{f/f}$) were provided by Dr. Laurie Glimcher (Harvard School of Public Health, Boston, MA). The mice were crossed with the CD19-Cre strain (CD19-Cre/XBP-$1^{f/f}$), provided by Dr. H. Ploegh. All mice were kept in the specific pathogen-free facility of the Hebrew University. All animal studies were conducted in accordance with the Principles of Laboratory Animal Care published by the National Institutes of Health. The Ethical Committee for Animal Use of Hadassah and the Faculty of Medicine reviewed protocols for Animal Welfare.

Cell culture and cell lines

Mature B cells were purified from mouse splenocytes by magnetic depletion with anti-CD43 (Miltenyi Biotec). Cells were plated at 1.5×10^6 cells/ml in complete medium containing RPMI 1640 (Invitrogen) supplemented with 10% FBS (Biological Industries), 2 mM glutamine, 50 U/ml penicillin, 50 μg/ml streptomycin, 50 μM β-ME, 25 mM 1× nonessential amino acids, and 1 mM sodium pyruvate (Biological Industries). i29μ^+ cells were propagated in the same B cell medium. 293T HEK cells were maintained in DMEM (Invitrogen) supplemented with 10% FCS, 2 mM glutamine, 50 U/ml penicillin, and 50 μg/ml of streptomycin (Biological Industries). CFSE dilution was performed by using a CellTrace CFSE cell proliferation kit (Molecular Probes) according to the manufacturer's instructions.

Metabolic labeling of cells to measure de novo [^{3}H]ceramide synthesis

[^{3}H]Ceramide synthesis was measured in cultured B cells as previously described (22), with some modifications. Briefly, primary B cells, treated with or without LPS for 3 days, were incubated with 0.33 μCi/ml [4,5-^{3}H]sphinganine/3.5 μM sphinganine for 20 min. The reaction was terminated by addition of methanol. Lipids were extracted (23) and separated by thin layer chromatography using chloroform/methanol (50:3.5 (v/v)) as the developing solvent [^{3}H]ceramide was visualized using a phosphorimager screen (Fuji) and recovered from the thin layer chromatography plates by scraping the silica directly into scintillation vials, and quantified by liquid scintillation counting.

Retrovirus production

XBP-1s was cloned into the pMIG MSCV vector harboring an internal ribosomal entry site-GFP element. Viral particles were made in 293T HEK cells by triple transfection of the retroviral vectors pMD-gag-pol and pVSV-G in a 2:1:1 ratio using Effecten (Qiagen). Analysis of positive GFP-expressing gels was done by flow cytometry.

Metabolic labeling, pulse-chase analysis, and immunoprecipitation

Pulse labeling and immunoprecipitation were performed as described previously (24). Briefly, after starvation in methionine/cysteine-free DMEM (Biological Industries) for 45 min, cells were metabolically labeled with [^{35}S]methionine/cysteine (7.5 mCi/500 μl) (Amersham Biosciences) at 37°C for 20 min. In pulse-chase, cells were metabolically labeled as above and were chased in 3 ml of chase medium containing complete B cell medium supplemented with an excess of nonradiolabeled cysteine/methionine. Cells were then lysed in 1% SDS, which was diluted by addition of 1.5 ml of lysis buffer (50 mM Tris (pH 8), 200 mM NaCl, 20 mM $MgCl_2$, and 1% Nonidet P-40, 3 μl/ml normal rabbit serum, 10 μl/ml 0.1% BSA, and protease inhibitors). Nonspecific protein binding was removed by addition of protein A beads (ADAR BioTech). Immunoprecipitation was performed using the indicated Abs. Immunoprecipitates were analyzed by 12% SDS-PAGE, followed by autoradiography.

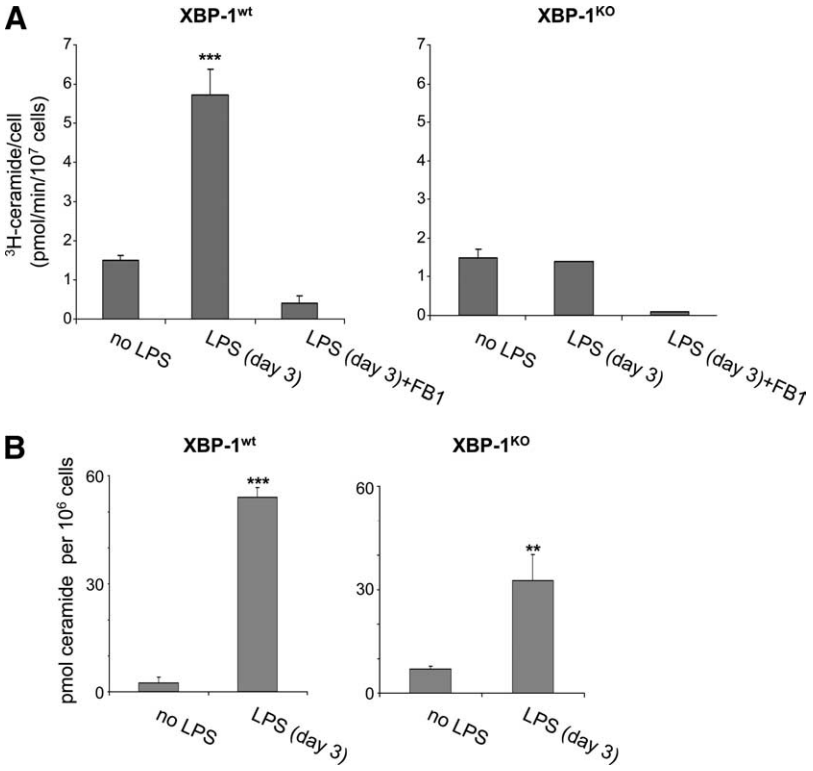

FIGURE 1. XBP-1 promotes the synthesis of ceramides. *A*, B cells were isolated from a pool of two to three spleens of either XBP-1^{wt} or XBP-1^{KO} mice. Cells (10^7) were washed with PBS, pulse-labeled with [^{3}H]sphinganine, washed, and kept frozen at −80°C until the end of the experiment. The remainder of the cells was cultured for 3 days in the presence of LPS, washed, and pulsed-labeled in the same manner. At day 3, FB1 (30 μM) was added 4 h before the pulse to validate the TLC separation of ceramides. The experiment was repeated three times. Bars represent the SD. *B*, Total ceramide content was quantified by mass spectroscopy. Shown is the average of two independent analyses. Each analysis was assayed in triplicates. Bars represent the SD of all measurements.

Reverse transcriptase PCR and real-time PCR analyses of XBP-1 splicing

Total RNA was isolated using Tri-Reagent (Sigma-Aldrich), and 1 μg was converted into cDNA using first-strand synthesis kit (Fermentas) with random primers. Real-time PCR was performed using the Absolute Blue SYBR Green mix (ABgene) on an MxPro real-time PCR device (Stratagene). Quantitative PCR analysis for total XBP-1 and XBP-1s was performed using the conditions in Back et al. (25). The Ubc gene was used as a reference gene (Ubc forward primer, 5′-CAG CCG TAT ATC TTC CCA GAC T-3′; Ubc reverse primer, 5′-CTC AGA GGG ATG CCA GTA ATC TA-3′). Splicing of XBP-1 was analyzed using a previously published protocol (24).

Nuclear magnetic resonance (NMR) spectroscopy

Cells were collected and washed twice with 0.9% NaCl (w/v). A mixture of cold methanol, chloroform, and distilled water were added to the washed pellet in a ratio of 1:1:1, and the samples were subsequently vortexed and incubated overnight at 4°C. The organic lower phase was separated, washed with 1 ml of 0.2 M KCl, and incubated overnight at 4°C. The upper phase was discarded and the lower phase evaporated under N_2. Immediately before analysis, the extracts were dissolved in 700 μl of deuterochloroform with 1 mM triethylphosphate as a standard, and K_4-EDTA (0.2 M)/methanol (1:4 (v/v)) was added in ratio of 2:1 (v/v). Samples were stirred and incubated for phase separation and analyzed by NMR spectrometry (Varian Inova 500). The NMR spectrometer was operated at 121 MHz for ^{31}P in a 60° flip angle, delay time 2 s, number of points 64,000, and temperature of 20°C. Signals were fully relaxed at these conditions. For each spectrum, 2800 pulses were collected. Chemical shift data are reported relative to PtdCho. Signals were quantified relative to the signal of 1 mM triethylphosphate and normalized to the number of cells. Two parameters for each of the phosphodiester-containing lipids were calculated: 1) the total amount of each, by calculating the signal of the phospholipid vs the signal of a standard in a given concentration; 2) the abundance of each of the phospholipids relative to the other, by calculating the signal of the phospholipid relative to the total signal (26). Lipids that do not contain a phosphodiester linkage, such as ceramide and cholesterol, do not contribute to the signal.

Mass spectrometry analysis of ceramide and SM

Primary B cells were treated with LPS for 3 days and collected at days 0 and 3 by centrifugation, washed twice with ice-cold PBS, and lyophilized. The samples were spiked with an SL internal standard mixture (Avanti Polar Lipids) and then extracted and analyzed by LC electrospray ionization-MS/MS. Analyses by electrospray ionization-MS/MS were conducted using a PE-Sciex API 3000 triple quadrupole mass spectrometer and an ABI 4000 quadruple-linear ion trap mass spectrometer as described previously (27).

Results

De novo ceramide biosynthesis is induced in the course of PC differentiation in an XBP-1-dependent fashion

Activation of naive splenic B cells in vitro with TLR agonists, such as LPS or CpG, recapitulates many of the features seen for PC differentiation in vivo. This includes the expansion of the ER, induction of XBP-1 mRNA splicing, preferential production of mRNA encoding the secreted μ-chains, and consequently a vast increase in the level of sIgM synthesis and secretion (28, 29). As wild-type mice, we used the recently generated conditional XBP-1 knockout mice (XBP-1$^{f/f}$, referred to as XBP-1^{wt}), which were not crossed to a Cre deleter strain (30). Specific deletion of XBP-1 in B cells was achieved by crossing XBP-1$^{f/f}$ mice with the CD19-Cre strain (CD19-Cre/XBP-1$^{f/f}$, referred to as XBP-1^{KO}) (31). Splenic B cells were isolated from XBP-1^{wt} mice and [^{3}H]ceramide de novo synthesis was measured at day 0 and after 3 days in the presence of LPS. On a per cell basis, [^{3}H]ceramide synthesis was increased ~3.5-fold upon LPS stimulation (Fig. 1*A*, *left panel*). In splenic B cells from XBP-1^{KO} mice, the induction of [^{3}H]ceramide synthesis was largely abolished (Fig. 1*A*, *right panel*). FB1 was added to validate the separation of ceramides by TLC.

To support these results we analyzed the steady-state amount of ceramides by mass spectrometry. Ceramide levels in wt B cells increased by 21-fold in response to LPS activation, but increased significantly less (i.e., 4.7- fold) in XBP-1-deficient B cells (Fig. 1*B*). The initial level of ceramides in the naive B cells was higher in the XBP-1^{KO} mice than in the XBP-1^{wt} mice. These results suggest that ceramide levels increase dramatically in the course of plasma cell differentiation in an XBP-1-dependent manner. It is

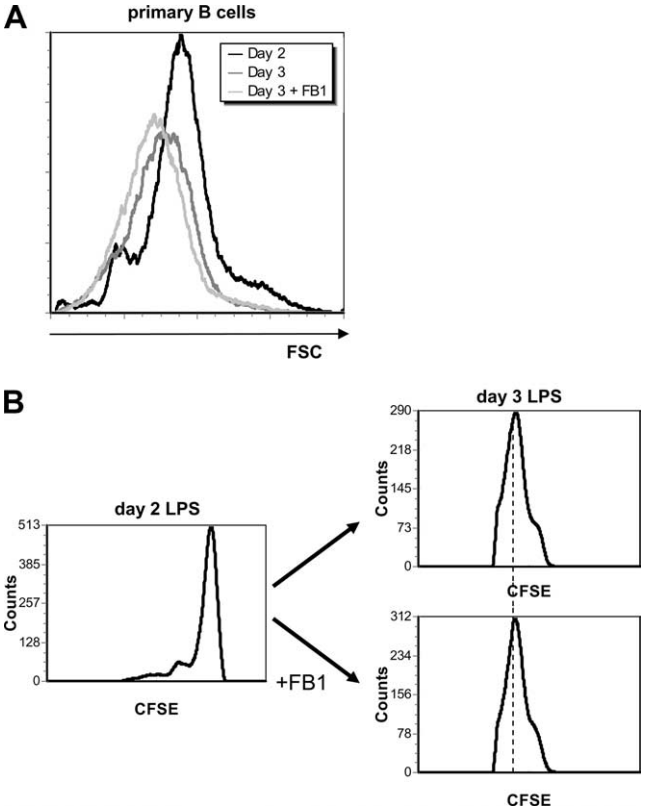

FIGURE 2. Addition of FB1 blocks ER expansion in the course of PC differentiation without affecting cell proliferation. *A*, B cells were extracted from a pool of two to three mouse spleens. Cells were cultured for 48 h in the presence of LPS. FB1 (30 μM) or DMSO was added for an additional 24 h. FCS of the cells, as an indication for cell size, was measured by flow cytometry. Shown is a representative experiment out of three independent repetitions. *B*, B cells were isolated as in *A*. After 48 h in the presence of LPS, 20×10^6 cells were labeled with CFSE and divided into two dishes. One was treated with FB1 (30 μM), and the second was treated with DMSO as a control. Samples were taken at days 2 and 3 and analyzed by flow cytometry for CFSE levels.

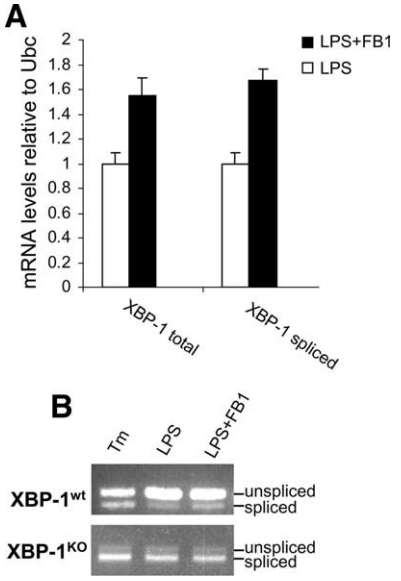

FIGURE 3. Addition of FB1 does not inhibit XBP-1 splicing. B cells were isolated from mouse spleens and treated with LPS for 48 h. FB1 was added (30 μM) for 24 h. Total RNA was extracted using the TriReagent, and cDNA was generated. XBP-1 splicing was measured using RT-PCR (*B*) and by quantitative PCR for total and the spliced form of XBP-1 (*A*). Shown are the results of three independent analyses.

noteworthy that the attenuation in ceramide synthesis measured in the XBP-1^{KO} cells is not a result of impaired proliferation, as both cell types proliferate similarly in response to LPS stimulation (data not shown).

Inhibition of de novo ceramide synthesis impairs the size expansion of plasma cells but does not affect their proliferation

To determine the relationship between de novo ceramide synthesis and PC differentiation, we analyzed the size of primary B cells isolated from spleens of XBP-1^{wt} mice after exposure to LPS. Typically, the size of LPS- or CpG-activated B cells, as assessed by the forward light scatter channel (FSC) in the flow cytometer, is reduced between days 2 to 3 of stimulation, most likely as a result of their rapid proliferation. We previously showed that the absence of XBP-1 confers smaller forward scatter starting from day 3 of stimulation, a time that immediately follows the peak of XBP-1 mRNA splicing (24). Thus, FSC measurement at day 3 of LPS-treated B cells may reflect XBP-1-dependent ER expansion. Therefore, we decided to focus on the effect of ceramide synthesis on B cell size at this time frame.

To ensure that the PC program is not compromised by complete depletion of ceramides, we first treated cells for 48 h with LPS to initiate proliferation and differentiation, and then FB1 was added for an additional 24 h while maintaining LPS in the culture. These conditions did not result in toxicity as assessed by propidium iodide staining (not shown). Flow cytometric analysis of live cells at day 3 demonstrated reduced FSC when treated with FB1 relative to control (Fig. 2*A*). This may result from either a block in ER expansion or inhibition of proliferation. Using a CFSE dilution assay, we observed normal proliferation (Fig. 2*B*). We conclude that the reduction in cell size is most likely due to a failure in ER expansion, similar to what we previously reported for XBP-1-deficient B cells (24).

A possible mechanism for the reduction in ER expansion may be the inhibition of XBP-1 splicing by FB1 treatment. To test this possibility we performed quantitative and RT-PCR analyses for spliced and total XBP-1 mRNA on FB1-treated and control cells. We saw that FB1 treatment did not impair the splicing of XBP-1. In fact, we consistently observed an enhancement of both the total mRNA levels of XBP-1 and its spliced form (Fig. 3*A*). We also performed this analysis on XBP-1-deficient B cells, which exhibit a high level of constitutive splicing of the mRNA owing to the lack of the derived protein. We saw no inhibition of XBP-1 splicing by FB1 even under these conditions (Fig. 3*B*). We conclude that FB1 affects ER expansion in a mechanism that does not involve XBP-1.

Inhibition of ceramide synthase by FB1 impairs N*-linked glycosylation in LPS-treated but not in naive B cells*

To further explore the mechanism by which FB1 blocks the expansion of the ER, we pulse-labeled cells with ^{35}S-methionine and followed the repertoire of newly synthesized proteins by SDS-PAGE. We noticed that the prominent band at ~73 kDa, which represents mature μ-chains (mark by arrow), changed its mobility (Fig. 4*A*). This experiment suggested that secreted μ-chains were modified differently in FB1-treated cells, possibly bearing altered *N*-linked glycans, or other peptide backbone modifications of newly synthesized μ-chains. To directly address the effects of FB1 on *N*-linked glycosylation, we pulse-labeled 3 day LPS-treated primary B cells with FB1. μ-Chains were immunoprecipitated and analyzed by SDS-PAGE. Treatment with FB1 caused a reduction

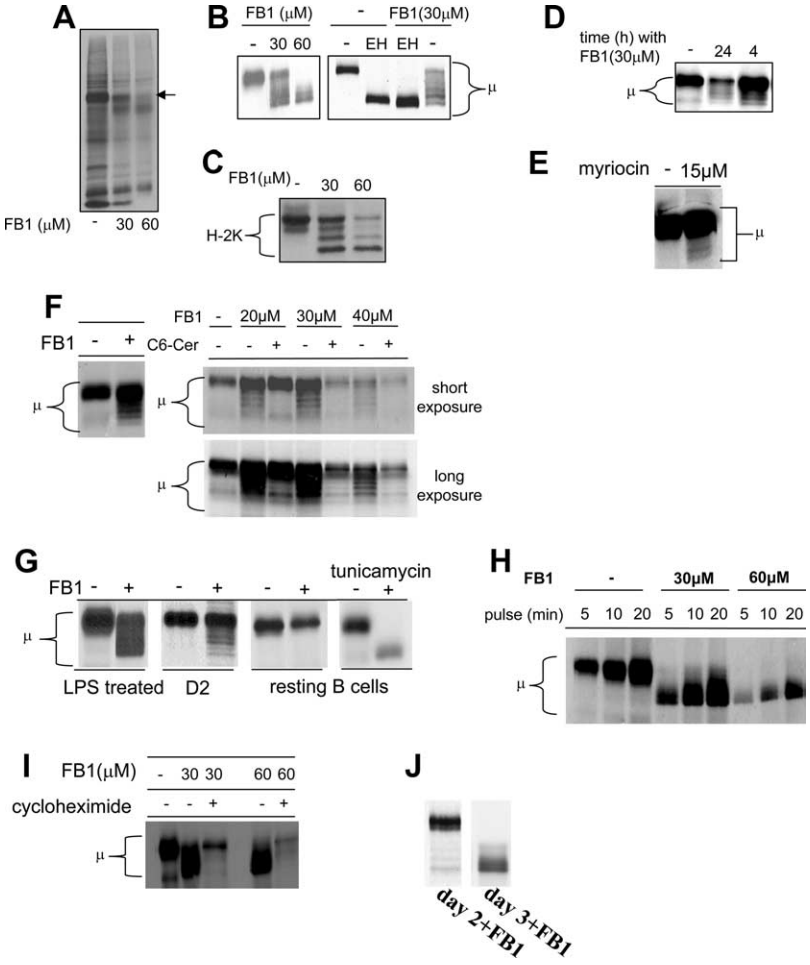

FIGURE 4. Inhibition of ceramide synthesis impairs *N*-linked glycosylation in plasma cells but not in naive B cells. In all experiments, unless otherwise indicated, B cells were extracted from mouse spleens and treated for 48 h with LPS. FB1 at the indicated concentration was added for an additional 24 h. Cells were pulse-labeled with ^{35}S-methionine for 20 min. *A*, Total lysates of pulse-labeled cells were analyzed by SDS-PAGE. μ-Chains are marked by the arrow. *B* and *C*, Cells were pulse-labeled, lyzed in 1% SDS, and lysates were diluted with lysis buffer. μ-Chains (*B*) or H-2K (*C*) were immunoprecipitated by their respective Abs. Immunoprecipitates, treated or not with endoglycosidase H (EH) to remove the glycans, were analyzed by SDS-PAGE (12%), followed by autofluorography. *D*, A time course for FB1 effect on μ-chain glycosylation. *E*, Myriocin, an upstream inhibitor of ceramide synthesis, was added for 24 h at the indicated concentration. *F*, Ceramides were added to overcome the FB1 block at 20 μM concentration for 6 h before pulse-labeling to allow their diffusion into the ER. *G*, Comparison of FB1 treatment on LPS-treated B cells, D2 (IgM-secreting hybridoma cells), and unstimulated B cells. Tunicamycin was added to inhibit *N*-linked glycosylation. *H*, The effect of pulse-labeling duration on μ-chain glycosylation state. *I*, CHX was added to inhibit protein synthesis. *J*, The degree of LPS stimulation correlates with defects in glycosylation. XBP-1^{wt} B cells were extracted and activated by LPS. At day 1 a portion of the cells was treated with FB1 and pulse-labeled at day 2 (*left panel*), while the rest were treated with FB1 at day 2 and pulse-labeled at day 3 (*right panel*). In all experiments, shown are typical autoradiograms of three repetitions.

in the molecular mass of μ-chains (Fig. 4*B*, *left panel*). Upon digestion with endoglycosidase H (EH), which cleaves high mannose *N*-linked glycans, both FB1-treated samples and controls converged into a single polypeptide. This indicates that the difference in migration on SDS-PAGE was a consequence of altered *N*-linked glycosylation (Fig. 4*B*, *right panel*).

Ig μ-chains are the major glycoprotein synthesized in LPS-treated B cells and thus may be more sensitive to alterations in ceramide levels than other glycoproteins. However, *N*-linked glycosylation is a general modification of proteins in the secretory pathway. To assess whether ceramide is required for glycosylation more generally, we analyzed the glycosylation pattern of class I MHC heavy chains. Similar to μ-chains, H-2K molecules exhibited a reduction in glycosylation upon FB1 treatment (Fig. 4*C*). We conclude that ceramide biosynthesis is a general requirement for *N*-linked glycosylation in LPS-stimulated B cells.

We were concerned that prolonged exposure of cells to FB1 may cause changes in ER physiology that are not directly related to its pharmacological activity as a CerS inhibitor. To address this concern, we performed three experiments. First, we analyzed *N*-linked glycosylation of μ-chains treated with FB1 for 4 h only. Although the magnitude of the phenomenon diminished, we could clearly detect partially glycosylated species after a short exposure to FB1 (Fig. 4*D*). Second, we exposed the cells to myriocin, which inhibits serine palmitoyl transferase, an enzyme upstream to CerS. As expected, myriocin was not as potent as FB1 because it does not block the salvage pathway of ceramide synthesis (i.e., the metabolism of sphingosine to ceramide) as does FB1. However, we could clearly detect μ-chains with altered glycosylation patterns (Fig. 4*E*). Finally, to directly prove that blocking CerS via FB1 is the cause of the defect in *N*-linked glycosylation, we attempted to bypass the effect of FB1 by incubating FB1-treated cells with exogenous short acyl chain ceramide (32, 33). C6-ceramide (20 μM) was added during the final 6 h of incubation with FB1 to allow trafficking into the ER, and cells were pulse labeled and μ-chain glycosylation was analyzed. It was not straightforward to normalize for incorporation of radioactive ^{35}S-methionine, and thus we decided to use different autoradiographic exposures to allow a comparison. Addition of C6-ceramide conferred a consistent improvement in the glycosylation pattern of μ-chains (Fig. 4*F*). Taken together, these experiments suggest a direct link between ceramide synthesis and *N*-linked glycosylation in plasma cells.

The effect of ceramide depletion on glycosylation was not restricted to LPS-treated primary B cells. Rather, exposure of D2 cells, a hybridoma that secretes high levels of IgM, to FB1 showed a similar phenotype, suggesting that fully differentiated PCs may be sensitive to FB1 (Fig. 4*G*). We did not discern any effect of FB1 treatment on naive splenic B cells, while short incubation with Tm, a blocker of *N*-linked glycosylation, resulted in the expected abrogation of glycosylation (Fig. 4*G*, *right panel*). These results indicate a preferential effect of FB1 on cells with a highly active secretory pathway, and they may suggest that only cells engaged in extensive ER biogenesis require de novo ceramide synthesis to support the glycosylation machinery.

The observed reduction in glycan size may be a consequence of the synthesis of LLOs that are shorter than normal, or of enhanced mannose trimming in the ER. We considered the latter possibility as unlikely because the effect was seen on proteins pulse-labeled

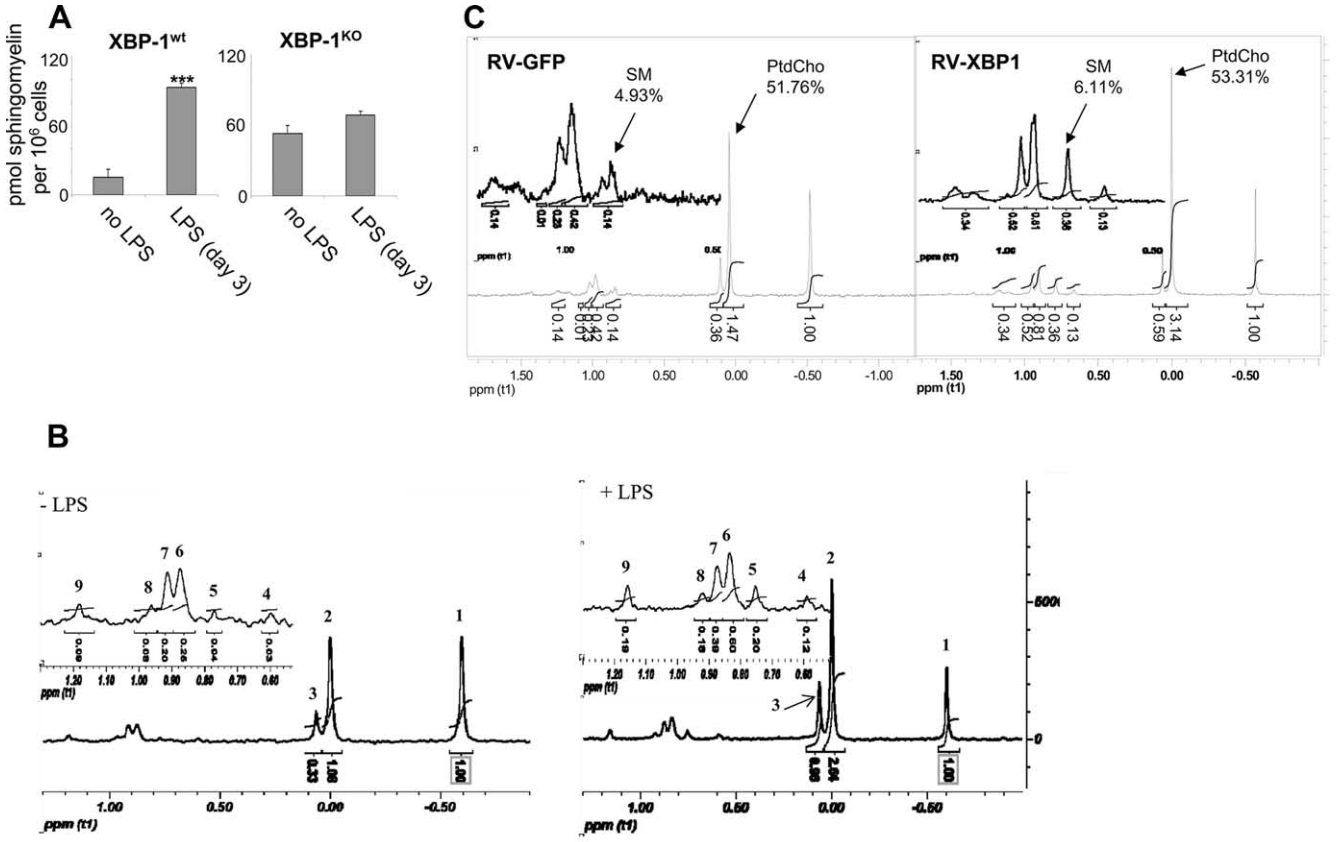

FIGURE 5. Sphingomyelin levels and its concentration relative to other phospholipids rise in the course of PC differentiation. *A*, B cells were isolated from a pool of two to three spleens of either XBP-1^{wt} or XBP-1^{KO} mice. A portion of the cells was cultured for 3 days in the presence of LPS, and the rest was immediately washed with PBS and kept at −80°C until the end of the experiment. After 3 days, the cells were washed and the same number of cells were washed and frozen. Cells were lyophilized and total SM content was quantified by mass spectroscopy. Shown is the average of two independent analyses. Each analysis was assayed in triplicates. *B*, i29μ^+ cells were cultured for 3 days in the presence of FB1. Cells (10^8) were washed and total lipids were extracted and analyzed by ^{31}P-NMR. Each of the peaks represents the level of the corresponding phospholipids as shown in Tables I and II. Peak no. 5 represents SM, and peak no. 2 represents PtdCho. *C*, 293T HEK cells were transfected with a vector that encodes XBP-1s. An IRES-GFP element was used to monitor the efficiency of expression. An empty IRES-GFP construct was used as a control. NMR analysis was performed as before. Indicated by arrows the peaks of SM and PtdCho.

for a short time (10–20 min), whereas mannose trimming is a slower process. Inclusion of kifunensine, an α-mannosidase inhibitor, did not affect the FB1-induced glycosylation defect (not shown). To further address this possibility, we pulse-labeled the cells for extended periods of time. If mannose trimming were responsible for the aberration in glycosylation, we would expect that prolonged pulse-labeling would exacerbate the defect in glycosylation. Rather, we saw no such trend (Fig. 4*H*). This indicates that the defect in glycosylation is a consequence of addition of shorter and/or fewer glycans, rather than enhanced glycan trimming. Hence, our data support a model in which the absence of ceramides probably confers a slower rate of LLO synthesis or inefficient transfer thereof. When the rate of glycoprotein synthesis exceeds the time needed to build the fully glycosylated LLOs, glycoproteins will be decorated with smaller glycans. We assume that LLO synthesis is the limiting factor in protein glycosylation. Indeed, when cells are incubated in the presence of low glucose concentrations, *N*-linked glycans are smaller than normal (26). Inhibition of protein synthesis either by PERK, as induced by conditions of ER stress, or artificially with cycloheximide (CHX) largely alleviated this phenotype, confirming that the rate-limiting step in protein glycosylation is LLO synthesis (34).

We therefore tested whether inclusion of CHX could correct the impairment in *N*-linked glycosylation. Primary B cells were activated for 3 days and FB1 was added during the final 24 h of stimulation. At the end of day 3, cells were treated with CHX for 50 min at concentrations that reduce protein synthesis by ~80%, as determined by TCA precipitation of pulse-labeled cells. Cells were then labeled in the presence of CHX and μ-chains were recovered by immunoprecipitation. Regardless of the concentration of FB1, treatment with CHX corrected the defect in glycosylation (Fig. 4*I*), suggesting that the imbalance between protein and LLO synthesis rates accounts for impaired glycosylation. This is supported by the fact that sensitivity to FB1 increased as the cells became more activated (Fig. 4*J*).

Several autoimmune diseases, such as rheumatoid arthritis and certain types of Ig deposition disorders, are associated with the appearance of Ig that is decorated with glycans of reduced size. The mechanism responsible for the generation of such underglycosylated Ig molecules is still not known. The SDS-PAGE profiles of these pathologic Ig molecules is highly reminiscent of what we observed for FB1-treated B cells (35, 36), strengthening the notion of a potential link between the two phenomena.

These observations prompted us to check whether underglycosylated μ-chains generated by FB1 treatment can be secreted. To this end, we conducted a pulse-chase analysis in which μ-chains were immunoprecipitated from the supernatants after 4 h of chase,

Table I. *SM is induced relative to glycerophospholipids in the course of PC differentiation*[a]

	Amount Relative to Standard (1) (AUC_l/AUC_s) per 10^8 Cells		
	Untreated	LPS (3 days)	LPS/Untreated
Phosphatidylcholine (2)	0.819	1.631	1.99*
Plasmalogen phosphatidylcholine (3)	0.324	0.726	2.24*
Phosphatidylinositol (4)	0.023	0.067	2.91*
Sphingomyelin (5)	0.023	0.134	5.82*
Phosphatidylserine (6)	0.157	0.359	2.28*
Phosphatidylethanolamine (7)	0.135	0.203	1.50*
Plasmalogen phosphatidylethanolamine (8)	0.041	0.077	1.87*
Cardiolipin (9)	0.044	0.102	2.31*

[a] i29μ^+ cells were stimulated by LPS for 3 days. Indicated are the average area under the curve (AUC) of the indicated lipid (AUC_l) to that of the standard (AUC_s) of three independent ^{31}P-NMR analyses of day 3 LPS and nontreated cells. Phospholipids are numbered according to the peak as shown in Fig. 5*B*. The amount relative to the standard (peak no. 1) is indicated. *, $p < 0.05$.

Table II. *The concentration of SM is increased relative to glycerophospholipids*[a]

	% Relative to Total Signal ($AUC_l/\Sigma AUC_{2-9}$)		
	Untreated	LPS (3 days)	LPS/Untreated
Phosphatidylcholine (2)	52.59	49.93	0.95
Plasmalogen phosphatidylcholine (3)	20.55	22.49	1.09
Phosphatidylinositol (4)	1.51	2.01	1.33
Sphingomyelin (5)	1.52	4.14	2.72*
Phosphatidylserine (6)	9.74	9.97	1.02
Phosphatidylethanolamine (7)	8.23	5.69	0.69
Plasmalogen phosphatidylethanolamine (8)	2.75	2.29	0.83
Cardiolipin (9)	2.75	2.83	1.03

[a] As in Table I. The area under the curve of a specific lipid (AUC_l) relative to total signal (cumulative area under the curve of peak nos. 2–9, ΣAUC_{2-9}) is indicated. *, $p < 0.05$.

the time needed for secretion of IgM (24). We observed that FB1 treatment neither prevented the secretion of the underglycosylated IgM (supplemental Fig. 1*A*[4]), nor the association with the L chain (supplemental Fig. 1*B*). We conclude that modification by *N*-linked glycans is not a precondition for either folding of the μ-chain, association with the L chain, or secretion of IgM. These observations are in agreement with analysis of IgM secretion in the presence of the glucosidase inhibitor deoxynojirimycin, which interferes with glycan addition to nascent μ-chains, but not with IgM secretion (37).

Induction of de novo ceramide biosynthesis leads to an increase in the levels of sphingomyelin

Treatment of B cells with LPS enhances the levels of PtdCho by ~2-fold (12). Ceramide synthesis was enhanced by >3.5-fold, and its total levels increased by ~25-fold (Fig. 1, *A* and *B*, respectively). These results suggest that in the course of PC differentiation there may be an overall enrichment not only of ceramide itself, but also of its downstream metabolites. To address this question, we examined levels of SM, which is synthesized directly from ceramide. Mass spectroscopy analysis of SM levels indicated a 5-fold increase. This up-regulation was diminished in the absence of XBP-1 (Fig. 5*A*).

To quantitatively account for the level of SM relative to all other phospholipids we extracted total cellular lipids and analyzed them by ^{31}P-NMR. Because this method requires a large number of cells (~10^{10} in the case of naive B cells), we performed the analysis on i29μ^+ B lymphoma cells, which respond to LPS stimulation in a similar fashion to primary B cells and show similar sensitivity to FB1 treatment (see supplemental Fig. 2) (8). At first we compared unstimulated i29μ^+ cells to cells treated for 3 days with LPS. As expected, all phospholipids showed an increase upon LPS stimulation. We confirmed that PtdCho was increased by ~2-fold (12). Intriguingly, SM, the only ceramide metabolite that contains a phosphodiester bond, was increased by almost 6-fold (Fig. 5*B* and Table I). Analysis of the relative abundance of the different phospholipids revealed no significant change for PtdCho. In fact, SM was the only phospholipid whose concentration increased (Table II). These data suggest that although the amount of phospholipid per cell is up-regulated upon LPS treatment, their concentrations are carefully regulated. An exception is SM, whose increased levels appear more than those required for homeostatic membrane expansion.

To assess the role of XBP-1 in the control of SM levels, we compared 3 day LPS-treated XBP-1^{wt} to XBP-1^{KO} B cells. Levels of PtdCho were reduced by ~16% in the absence of XBP-1 (Table III). However, the relative concentration of PtdCho remained unaffected by the absence of XBP-1 (Table IV). This reinforces the notion that the relative abundance of PtdCho in the membrane is carefully regulated in the course of PC differentiation. In contrast to PtdCho, the SM level was reduced by >50% in the absence of XBP-1 (Table III). Moreover, its relative abundance was reduced to a similar level (Table IV). Finally, to assess whether XBP-1s is sufficient to promote the generation of SM when overexpressed, we transduced 293T cells with a retrovirus that encodes XBP-1s. XBP-1s transfectants and their vector controls were propagated, harvested, and analyzed by ^{31}P-NMR. Although not all 293T cells were transduced with the XBP-1s-encoding viruses, we consistently observed that SM was enriched in XBP-1s-expressing cells (Fig. 5*C*). Based on the mass spectrometry data for ceramides and SM levels, the de novo ceramide synthesis measurements, and the NMR analysis for SM we conclude that in the course of PC differentiation XBP-1 strongly induces pathways of sphingolipid biosynthesis.

Table III. *SM is induced in an XBP-1-dependent manner relative to glycero-phospholipids in the course of PC differentiation*[a]

	Amount Relative to Standard (1) (AUC_l/AUC_s) per 10^8 Cells		
	XBP-1^{wt}	XBP-1^{KO}	wt/KO
Phosphatidylcholine (2)	0.781	0.678	1.16*
Plasmalogen phosphatidylcholine (3)	0.168	0.169	1.05
Phosphatidylinositol (4)	0.022	0.020	0.93
Sphingomyelin (5)	0.036	0.026	1.62*
Phosphatidylserine (6)	0.200	0.152	1.33*
Phosphatidylethanolamine (7)	0.122	0.138	0.86
Plasmalogen phosphatidylethanolamine (8)	ND	ND	ND
Cardiolipin (9)	0.020	0.034	0.92

[a] B cells of wt or XBP-1^{KO} mice were stimulated by LPS for 3 days. Indicated are the average area under the curve (AUC) of the indicated lipid (AUC_l) to that of the standard (AUC_s) of three independent ^{31}P-NMR analyses of day 3 LPS from both genotypes. The amount relative to the standard (peak no. 1) is indicated. *, $p < 0.05$.

[4] The online version of this article contains supplemental material.

Table IV. *The concentration of SM is increased relative to glycero-phospholipids in an XBP-1-dependent manner*[a]

	% Relative to Total Signal ($AUC_l/\Sigma AUC_{2-9}$)		
	XBP-1^{wt}	XBP-1^{KO}	wt/KO
Phosphatidylcholine (2)	57.06	57.07	1.00
Plasmalogen phosphatidylcholine (3)	12.37	13.58	0.92
Phosphatidylinositol (4)	1.62	1.46	0.79
Sphingomyelin (5)	2.85	2.00	1.53*
Phosphatidylserine (6)	13.69	11.92	1.15*
Phosphatidylethanolamine (7)	7.83	10.60	0.74*
Plasmalogen phosphatidylethanolamine (8)	ND	ND	ND
Cardiolipin (9)	2.13	2.87	0.78

[a] As in Table III. The area under the curve of a specific lipid (AUC_l) relative to total signal (cumulative area under the curve of peaks no. 2–9, ΣAUC_{2-9}) is indicated. *, $p < 0.05$.

Discussion

The conversion of mature B cells into Ab-secreting cells involves a dramatic modulation of all cellular components. The early response to LPS causes an up-regulation in the cellular demand for energy, while later the secretory pathway is remodeled to allow the successful accommodation of the copious amount of glycoproteins destined for secretion (8). In contrast to the proteome, the "lipidome" associated with this remarkable differentiation is less well understood.

Thus far, most effort has been invested in understanding how levels of PtdCho and phosphatidylethanolamine are regulated, as these lipids are major components of the ER. To account for the role of XBP-1 in ER biogenesis, XBP-1s was ectopically overexpressed in fibroblasts (7, 11). This model was compared with a more physiological setting in which the differentiation of naive B cells into Ab-secreting cells was followed (12). In both models, PtdCho synthesis was significantly increased by elevation of CCTα activity, but by different mechanisms. In fibroblasts, XBP-1s promoted the transcription of CCTα, but in the course of PC differentiation CCTα levels increase due to stabilization of the protein. This disparity should caution against general conclusions when comparing models of enforced ER biogenesis vs physiological ER biogenesis.

Because sphingolipids are an important component of lipid rafts, which are associated with many signaling cascades, including that of the BCR and Toll-like receptors (38, 39), we investigated their contribution to PC differentiation. We also asked whether XBP-1 plays a role in the metabolism of sphingolipids. We saw that de novo ceramide synthesis and ceramide levels were strongly induced upon LPS stimulation. This induction was much stronger than that which was reported for PtdCho (Fig. 1) (12). Moreover, the dependency of the up-regulation of ceramide biosynthesis on XBP-1 may indicate that ceramide biogenesis is an element of the PC differentiation program, the importance of which awaits further characterization.

The strong induction of ceramide biosynthesis in the course of PC differentiation affects levels of ceramide metabolites. Indeed, we demonstrated a significant up-regulation of SM levels in an XBP-1-dependent manner. Moreover, SM was the major phospholipid whose levels increase relative to all other phospholipids, including PtdCho (Fig. 5). Although PtdCho is still the major component for the generation of more ER membrane, its up-regulation did not take place at the expense of other lipids. Thus, the relative amount of PtdCho in the membrane bilayer remained constant. In contrast, SM concentration increased by almost 3-fold, and perhaps the other sphingolipids that lack the phosphodiester moiety are also enriched in PCs (Tables I and II). SM is generated in the Golgi by transferring a phosphorylcholine residue from PtdCho to ceramide, catalyzed by SM synthase (40). It is likely that the elevated levels of SM are simply a result of an increase in levels of the substrates of SM synthase, namely ceramide and PtdCho. Whether inhibition of sphingomyelinase activities also plays a role in the accumulation of SM is not known. This suggests that PC membranes may be enriched in sphingolipids relative to less fully differentiated B cells. In light of this, our data call for a rigorous examination of sphingolipid content in PC membranes.

Upon activation with LPS, XBP-1-deficient B cells contain significantly less PtdCho than do wt cells, but the relative abundance of PtdCho in XBP-1$^{-/-}$ cells remains unaltered. SM was most sensitive to the XBP-1 deficiency, resulting in a net decrease of its levels (Tables III and IV). These results strengthen the hypothesis that XBP-1 is tightly linked to the sphingolipid biosynthetic pathway.

Depending on the cell type, sphingolipids contribute a varied amount to net lipid mass. This contribution can be substantial, such as in neurons. However, the concentration of sphingolipids in the ER membrane is low (reviewed in Ref. 41). Ceramide is generated in the ER, but it is rapidly transported by a combination of carrier proteins and vesicular transport to the Golgi apparatus where it is converted to SM and glycosphingolipids (42). This rapid trafficking ensures that at steady-state, only small amounts of ceramide are present in the ER itself. It was therefore surprising that a block in ceramide synthesis conferred a severe reduction in the cell size of PCs, which cannot be accounted for by the mere absence of ceramides from ER membranes (Fig. 2). This situation may well be analogous to the role of cholesterol, which is produced in the ER but is present at low concentrations within this cellular compartment. The fact that cholesterol is constantly kept at low concentrations in the ER is exploited by the ER quality control machinery to regulate the degradation of the 3-hydroxy-3-methylglutaryl (HMG)-CoA reductase, the classical example of "regulated ER associated degradation". When the local concentration of cholesterol is high, a conformational change in HMG-CoA reductase is sensed by the Hrd1/Hrd3 system, which results in the degradation of this key rate-limiting enzyme by the ubiquitin proteasome system (43). The physiological roles of ceramides in the ER membrane are poorly understood. Therefore, by analogy with cholesterol, it is tempting to speculate that ceramides also play a regulatory role in the ER membrane. Indeed, recent evidence indicates that when ER membranes are enriched with ceramides, but not with dihydro-ceramides, ER-to-Golgi trafficking is inhibited (44). We propose an additional role for ceramides in the control of protein *N*-linked glycosylation.

To identify any putative functional link between sphingolipids and PC differentiation, we blocked ceramide synthesis with FB1, a well-characterized ceramide synthase inhibitor (18). We demonstrated that FB1 impaired the typical ER expansion of LPS-activated B cells without inhibiting XBP-1 splicing (Figs. 2 and 3). Further biochemical investigation revealed an aberration in *N*-linked glycosylation in a manner distinct from that of Tm, an inhibitor of *N*-linked glycosylation. Tm blocks the transfer of *N*-acetylglucosamine-1-phosphate from UDP-*N*-acetylglucosamine to the dolichol lipid carrier, the first step in the synthesis of the LLOs (45). Thus, Tm exhibits an "all or none" effect when added to cells (24). At high concentrations it completely blocks *N*-linked glycosylation, while at lower concentrations a subset of newly synthesized proteins lacks glycans, whereas the glycosylation of the remainder occurs normally. Thus, a laddering of partially glycosylated species on SDS-PAGE is never observed for

Tm. FB1-treated cells exhibit a different pattern of glycosylation inhibition. At low concentrations of FB1, heterogeneity in the glycosylation pattern was observed, which yielded a diffuse migration pattern rather than a single distinct band. At concentrations that approximated 60 μM, *N*-linked glycosylation of μ-chains was severely blocked, but a sharp single band such as occurs upon Tm treatment was never observed (Fig. 4). Therefore, the mechanism by which FB1 affects glycosylation is probably different from that of Tm.

Why has the effect of FB1 on *N*-linked glycosylation not been reported in other cell types, and why does ceramide depletion affect glycosylation in LPS-activated but not in resting B cells? As B cells become more activated, their sensitivity to FB1 treatment increases (Fig. 4*J*). We speculate that in contrast to other cell types, the unique features of PC differentiation, such as the induction of ER membrane neogenesis and the steep acceleration in LLO synthesis (21), require continuous ceramide synthesis. Thus, the dynamic operation of the *N*-linked glycosylation machinery in PCs is somehow linked to de novo ceramide synthesis. *N*-linked glycosylation is enhanced by >20-fold upon LPS stimulation of B cells, due to enhanced synthesis of LLOs (21). Several steps in the synthesis of LLOs are augmented, including the synthesis of dolichol (46). The remarkable increase in the rate of glycosylation is the cumulative result of many enzymatic steps. Ceramides might play a regulatory role in several steps of the synthesis pathway of LLOs, rather than facilitating the actual oligosaccharide transfer to the nascent polypeptide chain. In support of this hypothesis is the fact that a general reduction in the rate of protein synthesis, as conferred by CHX, is sufficient to completely correct the aberration of glycosylation under ceramide depletion (Fig. 4).

If LLO synthesis is indeed reduced in the absence of ceramide synthesis, how does this regulation occur? By analogy with the role of ceramide in apoptosis, two alternative possibilities can be considered. One explanation may implicate the physical properties of ceramides in the ER membrane as being required for the LLO synthesis machinery and/or the recycling of dolichol. The other invokes a signaling cascade that is activated by ceramides, emanating from the ER and required for the acceleration of LLO synthesis. Concerning the first possibility, a causative link between ceramide and dolichol syntheses has not been identified. However, an inverse connection was reported in yeast. Ablation of CWH8, which blocks dolichol recycling in yeast, causes a strong defect in sphingolipid synthesis concomitant with a defect in *N*-linked glycosylation. Moreover, this defect was recapitulated by treatment with Tm (47). Thus, evidence linking sphingolipid biosynthesis to the machinery of *N*-linked glycosylation is only beginning to accumulate. Concerning the second possibility, protein kinase A was recently demonstrated to regulate *N*-linked glycosylation (48). Ceramides activate protein kinase A (49), but addition of an inhibitor of protein kinase A did not exhibit a phenotype similar to that evoked by treatment with FB1 (not shown). Additional experiments are needed to exclude or confirm the ceramide-protein kinase A axis as the underlying mechanism of this phenomenon.

Under-glycosylated Ig molecules, comprised of high mannose glycans that lack galactose residues, are frequently detected in the serum of rheumatoid arthritis patients. Moreover, the appearance of these Abs, mostly of the IgG isotype, correlates with disease severity and reverses in remission (35). The etiology of this phenomenon is not known. We investigated whether the defect in *N*-linked glycosylation of the μH chains as conferred by FB1 treatment results in the secretion of underglycosylted IgM or their arrest by the ER quality control machinery. Our findings indicated that the modulation of glycan composition did not abrogate the secretion (supplemental Fig. 1). This is not a general rule for all Ig molecules. While IgA molecules require glycosylation for proper trafficking in the secretory pathway (50), secretion of IgG molecules is impervious to the modification state of glycans (51). Our results suggest a physiological mechanism for the generation of underglycosylated Ig molecules.

In summary, our results imply a previously unknown role for ceramide biosynthesis as a key metabolic event downstream to XBP-1 in the process of PC differentiation. The up-regulation of this pathway above the typical homeostatic increase is required for ER expansion and is required to support protein *N*-linked glycosylation. This discovery may lay the foundation for a novel approach of drug therapy that will synergize with current treatments of PC-related diseases.

Acknowledgments

We would like to thank Dr. Ann-Hwee Lee for critically reviewing the manuscript. We thank Dr. Laurie Glimcher for providing the XBP-1$^{f/f}$ breeding pairs. We thank Dr. Hidde Ploegh for providing the CD19-Cre mice and valuable reagents.

Disclosures

The authors have no financial conflicts of interest.

References

1. Calame, K. L., K. I. Lin, and C. Tunyaplin. 2003. Regulatory mechanisms that determine the development and function of plasma cells. *Annu. Rev. Immunol.* 21: 205–230.
2. Klein, U., S. Casola, G. Cattoretti, Q. Shen, M. Lia, T. Mo, T. Ludwig, K. Rajewsky, and R. Dalla-Favera. 2006. Transcription factor IRF4 controls plasma cell differentiation and class-switch recombination. *Nat. Immunol.* 7: 773–782.
3. Shapiro-Shelef, M., K. I. Lin, L. J. McHeyzer-Williams, J. Liao, M. G. McHeyzer-Williams, and K. Calame. 2003. Blimp-1 is required for the formation of immunoglobulin secreting plasma cells and pre-plasma memory B cells. *Immunity* 19: 607–620.
4. Reimold, A. M., N. N. Iwakoshi, J. Manis, P. Vallabhajosyula, E. Szomolanyi-Tsuda, E. M. Gravallese, D. Friend, M. J. Grusby, F. Alt, and L. H. Glimcher. 2001. Plasma cell differentiation requires the transcription factor XBP-1. *Nature* 412: 300–307.
5. Iwakoshi, N. N., A. H. Lee, P. Vallabhajosyula, K. L. Otipoby, K. Rajewsky, and L. H. Glimcher. 2003. Plasma cell differentiation and the unfolded protein response intersect at the transcription factor XBP-1. *Nat. Immunol.* 4: 321–329.
6. Gass, J. N., N. M. Gifford, and J. W. Brewer. 2002. Activation of an unfolded protein response during differentiation of antibody-secreting B cells. *J. Biol. Chem.* 277: 49047–49054.
7. Sriburi, R., S. Jackowski, K. Mori, and J. W. Brewer. 2004. XBP1: a link between the unfolded protein response, lipid biosynthesis, and biogenesis of the endoplasmic reticulum. *J. Cell. Biol.* 167: 35–41.
8. van Anken, E., E. P. Romijn, C. Maggioni, A. Mezghrani, R. Sitia, I. Braakman, and A. J. Heck. 2003. Sequential waves of functionally related proteins are expressed when B cells prepare for antibody secretion. *Immunity* 18: 243–253.
9. Schroder, M., and R. J. Kaufman. 2005. The mammalian unfolded protein response. *Annu. Rev. Biochem.* 74: 739–789.
10. Shaffer, A. L., M. Shapiro-Shelef, N. N. Iwakoshi, A. H. Lee, S. B. Qian, H. Zhao, X. Yu, L. Yang, B. K. Tan, A. Rosenwald, et al. 2004. XBP1, downstream of Blimp-1, expands the secretory apparatus and other organelles, and increases protein synthesis in plasma cell differentiation. *Immunity* 21: 81–93.
11. Sriburi, R., H. Bommiasamy, G. L. Buldak, G. R. Robbins, M. Frank, S. Jackowski, and J. W. Brewer. 2007. Coordinate regulation of phospholipid biosynthesis and secretory pathway gene expression in XBP-1(S)-induced endoplasmic reticulum biogenesis. *J. Biol. Chem.* 282: 7024–7034.
12. Fagone, P., R. Sriburi, C. Ward-Chapman, M. Frank, J. Wang, C. Gunter, J. W. Brewer, and S. Jackowski. 2007. Phospholipid biosynthesis program underlying membrane expansion during B-lymphocyte differentiation. *J. Biol. Chem.* 282: 7591–7605.
13. Lee, A. H., E. F. Scapa, D. E. Cohen, and L. H. Glimcher. 2008. Regulation of hepatic lipogenesis by the transcription factor XBP1. *Science* 320: 1492–1496.
14. Futerman, A. H., and H. Riezman. 2005. The ins and outs of sphingolipid synthesis. *Trends Cell Biol.* 15: 312–318.
15. Futerman, A. H., and Y. A. Hannun. 2004. The complex life of simple sphingolipids. *EMBO Rep.* 5: 777–782.
16. Mathias, S., L. A. Pena, and R. N. Kolesnick. 1998. Signal transduction of stress via ceramide. *Biochem. J.* 335: 465–480.
17. Zhang, Y., B. Yao, S. Delikat, S. Bayoumy, X. H. Lin, S. Basu, M. McGinley, P. Y. Chan-Hui, H. Lichenstein, and R. Kolesnick. 1997. Kinase suppressor of Ras is ceramide-activated protein kinase. *Cell* 89: 63–72.
18. Wang, E., W. P. Norred, C. W. Bacon, R. T. Riley, and A. H. Merrill, Jr. 1991. Inhibition of sphingolipid biosynthesis by fumonisins: implications for diseases associated with *Fusarium moniliforme*. *J. Biol. Chem.* 266: 14486–14490.
19. Merrill, A. H., Jr., D. C. Liotta, and R. T. Riley. 1996. Fumonisins: fungal toxins that shed light on sphingolipid function. *Trends Cell Biol.* 6: 218–223.

20. Parodi, A. J. 2000. Protein glucosylation and its role in protein folding. *Annu. Rev. Biochem.* 69: 69–93.
21. Rush, J. S., E. C. Snow, and C. J. Waechter. 1987. Induction of glycoprotein biosynthesis in activated B lymphocytes. *Arch. Biochem. Biophys.* 259: 567–575.
22. Riebeling, C., J. C. Allegood, E. Wang, A. H. Merrill, Jr., and A. H. Futerman. 2003. Two mammalian longevity assurance gene (LAG1) family members, trh1 and trh4, regulate dihydroceramide synthesis using different fatty acyl-CoA donors. *J. Biol. Chem.* 278: 43452–43459.
23. Folch, J., M. Lees, and G. H. Sloane Stanley. 1957. A simple method for the isolation and purification of total lipides from animal tissues. *J. Biol. Chem.* 226: 497–509.
24. Tirosh, B., N. N. Iwakoshi, L. H. Glimcher, and H. L. Ploegh. 2005. XBP-1 specifically promotes IgM synthesis and secretion, but is dispensable for degradation of glycoproteins in primary B cells. *J. Exp. Med.* 202: 505–516.
25. Back, S. H., M. Schroder, K. Lee, K. Zhang, and R. J. Kaufman. 2005. ER stress signaling by regulated splicing: IRE1/HAC1/XBP1. *Methods* 35: 395–416.
26. Ting, Y. L., D. Sherr, and H. Degani. 1996. Variations in energy and phospholipid metabolism in normal and cancer human mammary epithelial cells. *Anticancer Res.* 16: 1381–1388.
27. Merrill, A. H., Jr., M. C. Sullards, J. C. Allegood, S. Kelly, and E. Wang. 2005. Sphingolipidomics: high-throughput, structure-specific, and quantitative analysis of sphingolipids by liquid chromatography tandem mass spectrometry. *Methods* 36: 207–224.
28. Stevens, R. H., B. A. Askonas, and J. L. Welstead. 1975. Immunoglobulin heavy chain mRNA in mitogen-stimulated B cells. *Eur. J. Immunol.* 5: 47–53.
29. Krieg, A. M., A. K. Yi, S. Matson, T. J. Waldschmidt, G. A. Bishop, R. Teasdale, G. A. Koretzky, and D. M. Klinman. 1995. CpG motifs in bacterial DNA trigger direct B-cell activation. *Nature* 374: 546–549.
30. Hetz, C., A. H. Lee, D. Gonzalez-Romero, P. Thielen, J. Castilla, C. Soto, and L. H. Glimcher. 2008. Unfolded protein response transcription factor XBP-1 does not influence prion replication or pathogenesis. *Proc. Natl. Acad. Sci. USA* 105: 757–762.
31. Rickert, R. C., J. Roes, and K. Rajewsky. 1997. B lymphocyte-specific, Cre-mediated mutagenesis in mice. *Nucleic Acids Res.* 25: 1317–1318.
32. Hu, W., R. Xu, G. Zhang, J. Jin, Z. M. Szulc, J. Bielawski, Y. A. Hannun, L. M. Obeid, and C. Mao. 2005. Golgi fragmentation is associated with ceramide-induced cellular effects. *Mol. Biol. Cell* 16: 1555–1567.
33. Jayadev, S., J. C. Barrett, and E. Murphy. 2000. Elevated ceramide is downstream of altered calcium homeostasis in low serum-induced apoptosis. *Am. J. Physiol.* 279: C1640–C1647.
34. Shang, J., N. Gao, R. J. Kaufman, D. Ron, H. P. Harding, and M. A. Lehrman. 2007. Translation attenuation by PERK balances ER glycoprotein synthesis with lipid-linked oligosaccharide flux. *J. Cell. Biol.* 176: 605–616.
35. Malhotra, R., M. R. Wormald, P. M. Rudd, P. B. Fischer, R. A. Dwek, and R. B. Sim. 1995. Glycosylation changes of IgG associated with rheumatoid arthritis can activate complement via the mannose-binding protein. *Nat. Med.* 1: 237–243.
36. Omtvedt, L. A., L. Royle, G. Husby, K. Sletten, C. M. Radcliffe, D. J. Harvey, R. A. Dwek, and P. M. Rudd. 2006. Glycan analysis of monoclonal antibodies secreted in deposition disorders indicates that subsets of plasma cells differentially process IgG glycans. *Arthritis Rheum.* 54: 3433–3440.
37. Peyrieras, N., E. Bause, G. Legler, R. Vasilov, L. Claesson, P. Peterson, and H. Ploegh. 1983. Effects of the glucosidase inhibitors nojirimycin and deoxynojirimycin on the biosynthesis of membrane and secretory glycoproteins. *EMBO. J.* 2: 823–832.
38. Chung, J. B., M. A. Baumeister, and J. G. Monroe. 2001. Cutting edge: differential sequestration of plasma membrane-associated B cell antigen receptor in mature and immature B cells into glycosphingolipid-enriched domains. *J. Immunol.* 166: 736–740.
39. Pfeiffer, A., A. Bottcher, E. Orso, M. Kapinsky, P. Nagy, A. Bodnar, I. Spreitzer, G. Liebisch, W. Drobnik, et al. 2001. Lipopolysaccharide and ceramide docking to CD14 provokes ligand-specific receptor clustering in rafts. *Eur. J. Immunol.* 31: 3153–3164.
40. Futerman, A. H., B. Stieger, A. L. Hubbard, and R. E. Pagano. 1990. Sphingomyelin synthesis in rat liver occurs predominantly at the *cis* and medial cisternae of the Golgi apparatus. *J. Biol. Chem.* 265: 8650–8657.
41. van Meer, G. 1998. Lipids of the Golgi membrane. *Trends Cell Biol.* 8: 29–33.
42. Hanada, K., K. Kumagai, N. Tomishige, and M. Kawano. 2007. CERT and intracellular trafficking of ceramide. *Biochim. Biophys. Acta* 1771: 644–653.
43. Gardner, R. G., A. G. Shearer, and R. Y. Hampton. 2001. In vivo action of the HRD ubiquitin ligase complex: mechanisms of endoplasmic reticulum quality control and sterol regulation. *Mol. Cell. Biol.* 21: 4276–4291.
44. Giussani, P., M. Maceyka, H. Le Stunff, A. Mikami, S. Lepine, E. Wang, S. Kelly, A. H. Merrill, Jr., S. Milstien, and S. Spiegel. 2006. Sphingosine-1-phosphate phosphohydrolase regulates endoplasmic reticulum-to-Golgi trafficking of ceramide. *Mol. Cell. Biol.* 26: 5055–5069.
45. Takatsuki, A., and G. Tamura. 1971. Effect of tunicamycin on the synthesis of macromolecules in cultures of chick embryo fibroblasts infected with Newcastle disease virus. *J. Antibiot.* 24: 785–794.
46. Crick, D. C., J. R. Scocca, J. S. Rush, D. W. Frank, S. S. Krag, and C. J. Waechter. 1994. Induction of dolichyl-saccharide intermediate biosynthesis corresponds to increased long chain *cis*-isoprenyltransferase activity during the mitogenic response in mouse B cells. *J. Biol. Chem.* 269: 10559–10565.
47. Pittet, M., D. Uldry, M. Aebi, and A. Conzelmann. 2006. The *N*-glycosylation defect of *cwh8*Δ yeast cells causes a distinct defect in sphingolipid biosynthesis. *Glycobiology* 16: 155–164.
48. Martinez, J. A., J. J. Tavarez, C. M. Oliveira, and D. K. Banerjee. 2006. Potentiation of angiogenic switch in capillary endothelial cells by cAMP: a cross-talk between up-regulated LLO biosynthesis and the HSP-70 expression. *Glycoconj. J.* 23: 209–220.
49. Cabral, L. M., M. Wengert, A. A. da Ressurreicao, P. H. Feres-Elias, F. G. Almeida, A. Vieyra, C. Caruso-Neves, and M. Einicker-Lamas. 2007. Ceramide is a potent activator of plasma membrane Ca^{2+}-ATPase from kidney-promixal tubule cells with protein kinase A as an intermediate. *J. Biol. Chem.* 282: 24599–24606.
50. Taylor, A. K., and R. Wall. 1988. Selective removal of alpha heavy-chain glycosylation sites causes immunoglobulin A degradation and reduced secretion. *Mol. Cell. Biol.* 8: 4197–4203.
51. Nuttall, J., J. K. Ma, and L. Frigerio. 2005. A functional antibody lacking *N*-linked glycans is efficiently folded, assembled and secreted by tobacco mesophyll protoplasts. *Plant Biotech. J.* 3: 497–504.